

Thermally induced morphological transition from lamella to gyroid in a binary blend of diblock copolymers

Shinichi Sakurai,^{a)} Hideo Umeda, Chizuko Furukawa, Hiroshi Irie, and Shunji Nomura
*Department of Polymer Science and Engineering, Kyoto Institute of Technology, Sakyo-ku,
Kyoto 606, Japan*

Hee Hyun Lee and Jin Kon Kim
*Department of Chemical Engineering and Polymer Research Institute, Pohang University of Science and
Technology, Pohang, Kyungbuk 790-784, Korea*

(Received 4 February 1997; accepted 3 December 1997)

We report an experimental result of the thermally induced morphological transition from lamellar to gyroid phase in a binary blend of polystyrene-*block*-polyisoprene (SI) diblock copolymers. Two SI copolymers employed in this study have almost the same molecular weights but different volume fractions of polystyrene (PS) block ($\phi_{PS}=0.26$ and 0.65). The blend was prepared by these two SI diblock copolymers and the overall volume fraction of PS block in the blend, ϕ_{PS} , was 0.58 . Time-resolved small-angle x-ray scattering (SAXS) experiments were conducted to reveal morphological structures as a function of temperature from 120 to 205 °C during the heating with a rate of 2 °C/min. It was observed from SAXS results that the lamellar phase (L) was found below 164 °C, the gyroid phase (G) above 188 °C, and the coexistence of L and G phases between these temperatures. The gyroid phase was confirmed by transmission electron micrograph. The transition from L to G phase is different from a thermally induced transition of kinetically locked morphology formed by the vitrification of the PS matrix, because it was also found by a separate SAXS experiment for the specimen annealed for long times in which the lamellar phase was stable up to 140 °C, which is well above the glass transition temperature of the PS block. A temperature sweep of SAXS experiment with a smaller heating rate was a useful method to roughly estimate the transition temperature. Moreover, it was found from this experiment that the position of the first-order peak does not change remarkably upon the transition. Although the thermoreversibility of the transition between L and G phases has not yet been confirmed, it does not necessarily mean that the lamellar morphology is not stable at lower temperatures. © 1998 American Institute of Physics. [S0021-9606(98)50610-1]

I. INTRODUCTION

Thermally induced morphological transition in a block copolymer provides an interesting and important knowledge for control of morphology.¹ Although some experimental results were reported recently,²⁻¹⁰ only little is revealed for the morphological transition, even for a neat diblock copolymer. Hajduk *et al.*⁸ have reported the morphological transition from lamella (L) to gyroid (G) phase for a polystyrene-*block*-polyisoprene (SI) sample with 37 wt. % polystyrene (PS) block and $M_w=27.4\times 10^3$ (weight-average molecular weight). They conducted careful experiments of small-angle x-ray scattering (SAXS) complementarily with transmission electron microscopy (TEM). Note here that the gyroid is newly discovered morphology which has $Ia\bar{3}d$ cubic symmetry of the space group.⁸ They further confirmed thermoreversibility for the transition between 100 and 160 °C. In accord with their result, thermodynamic stability of the gyroid phase is predicted by the self-consistent field theory.¹¹ They have also made a survey of the morphological states with the use of binary blends of this SI diblock with ho-

mopolystyrene or homopolyisoprene in the compositional range of 30–42 wt. % of PS blocks.⁸ In this range, the gyroid morphology was definitely confirmed.

A binary blend of diblock copolymers, $(A-B)_\alpha+(A-B)_\beta$, is another candidate for the control of morphology through control of an overall composition.¹² As compared to anionic polymerization of a neat block copolymer with a desired composition, it is more convenient and accurate to mix two different diblocks if the compositions of these individual diblocks are well characterized. Needless to say, the simplest way for the control of the overall composition is to blend A and/or B homopolymers with $A-B$ diblock copolymers, as Hajduk *et al.*⁸ have applied. However, we should be aware that macrophase separation often occurs in this case. Even if it is not the case, another complicated situation exists in the blend of $A-B$ and A (and/or B). Segregation of homopolymers in a lamellar microdomain space may take place and in turn the localized homopolymer layers unbind $A-B$ alternating lamellae.¹³ For instance, A homopolymer layers isolate a single B lamella. This is referred to as the unbinding transition.¹⁴ Such a situation is unfavored to morphological control through controlling the overall composition. Therefore, we chose binary blend of diblock copolymers as a

^{a)} Author to whom correspondence should be addressed.

TABLE I. Sample characteristics.

| Code name | ϕ_{PS}^1 | $M_n^2 \times 10^3$ | M_w/M_n^3 | Z^4 | Microstructure of PI ⁵ (mol %) | | |
|-----------|---------------|---------------------|-------------|-------|-------------------------------------------|-----------|-----|
| | | | | | cis-1,4 | trans-1,4 | 3,4 |
| SIZ-3 | 0.65 | 26.1 | 1.06 | 302 | 61 | 33 | 6 |
| SIZ-4 | 0.26 | 24.5 | 1.05 | 302 | 73 | 20 | 7 |

¹Volume fraction of polystyrene, analyzed by NMR.

²Number-average molecular weight measured by membrane osmometry.

³Polydispersity index of molecular weight, measured by GPC. (M_w denotes the weight-average molecular weight.)

⁴Reduced value of total degree of polymerization.

⁵Analyzed by NMR.

model for the morphological control. It was pointed out, however, that macroscopic phase separation occurs when the entire molecular weights of α and β are very different.¹⁵ Moreover, mimesis of the binary blends of diblocks was found to be imperfect,^{6,16} even if the entire molecular weights of α and β are similar. The morphological states of binary blends of diblocks strongly depend on the molecular weights and compositions of the respective copolymers, as also pointed out by the self-consistent field theory.^{17,18} Furthermore, anomalous temperature behavior was found for lamellae comprising α and β diblocks.¹⁹ Thus the binary blends of diblock copolymers are worth to intensively study. The primary interest of the binary blend of diblock copolymers is to see a morphological behavior by controlling the overall composition.

In the present paper, the thermally induced morphological transition from L to G is reported for the binary blend of diblock copolymers. The SI diblock copolymers were blended to prepare the overall composition (volume fraction of PS), ϕ_{PS} , 0.58 for which the gyroid morphology was found in our previous study.²⁰ Moreover, it was found that the lamellar morphology stable at a lower temperature is transformed into the gyroid morphology at a higher temperature. The transition was spontaneous upon heating the sample. This sample enables us to conduct in situ observation of the transition from L to G . Due to such an advantage, the present system is worth to study for understanding thermally induced morphological transition.

II. EXPERIMENT

The characteristics of the SI samples used were listed in Table I. Note that SIZ-3 and SIZ-4 have similar molecular weights (see the value of Z in Table I), but different composition (volume fraction of PS, ϕ_{PS}). Z denotes the reduced value of total degree of polymerization of the copolymer where effects of difference in the segment size for PS and PI (polyisoprene) are corrected for. Z is defined as

$$Z = (v_{PS}N_{PS} + v_{PI}N_{PI})/v_0, \quad (1)$$

with $v_0 = \sqrt{v_{PS}v_{PI}}$. v_0 , v_{PS} , and v_{PI} are molar volumes of the reference cell, PS, and PI segments, respectively. Note here that the values of v_K used were 107.2 and 81.9 cm³/mol for PS and PI, respectively, which were evaluated from the values of mass density 0.969 g/cm³ for PS and 0.830 g/cm³

for PI at 413 K.²¹ N_K designates degree of polymerization for K block ($K=PS$ or PI). Given amounts of two kinds of SI samples were dissolved into toluene with a total polymer concentration of ca. 5 wt. %. The toluene solution was poured into a petri dish and then the solvent evaporates gradually. The overall composition, ϕ_{PS} , was prepared to be 0.58 (82 vol % of SIZ-3 and 18 vol % of SIZ-4).

The SAXS measurements with synchrotron radiations were conducted at the BL-10C beam line of the Photon Factory in the Institute of High Energy Physics, Japan. The light source of this beam line is a bending magnet. The primary beam was monochromatized with a couple of Si(111) crystals at the wavelength of 0.1488 nm (the photon energy of x-rays is 8.33 keV) and then it was focused on a detector plane by a Pt-coated bent cylindrical mirror. A one-dimensional position sensitive proportional counter (PSPC) was used to detect intensities and was set vertically at a position of 1.9-m apart from the sample. Typical exposure time was chosen to be 5 min for our block copolymer samples of about 1 mm thickness.

The sample holder enables us to keep the samples at high temperatures up to 300 °C. At such a high temperature, leaking out of molten samples from the sample cell should be prevented. For this purpose, about 6- μ m-thick films of poly(ethylene terephthalate) (PET) were used as windows. The cast film of the sample was placed in the sample holder in such a way that the film normal is parallel to the path of the primary beam (so-called through view). We subtracted the scattering intensity of an empty cell with two pieces of thin PET films from that of samples by taking into account of transmittance of x-rays through the samples. A contribution of the thermal diffuse scattering (TDS) arising from the density fluctuations was further subtracted. Here, we approximated that the intensity at the high q region, where the scattering intensity is independent of q , is identical to the intensity level of TDS. Here, q stands for the magnitude of the scattering vector, defined as

$$q = (4\pi/\lambda)\sin(\theta/2), \quad (2)$$

with $\lambda (=0.1488$ nm) and θ being the wavelength of the incident x-rays and the scattering angle, respectively. Note that thus obtained scattering intensities were not converted to the absolute unit, since we do not necessarily need to know absolute intensities.

Some of synchrotron SAXS measurements were conducted at the 3C2 beam line at the Pohang Light Source (PLS), Korea.²² The primary beam was monochromatized with double Si(111) crystals at the wavelength of 0.1598 nm (the photon energy of x-ray is 7.76 keV) and then it was focused on a detector plane by a bent cylindrical mirror. A one-dimensional position sensitive detector (Diode-Array PSD; Princeton Instruments Inc.; Model ST-120) with the distance of each diode of 25 μ m was used.

III. RESULTS AND DISCUSSION

Figure 1 shows the SAXS profiles [$\log I(q)$ vs q] measured at room temperature for neat block copolymers of SIZ-3 annealed at 150 °C for 2 h and SIZ-4 annealed at 110 °C for 26 h, where $I(q)$ denotes the scattering intensity.

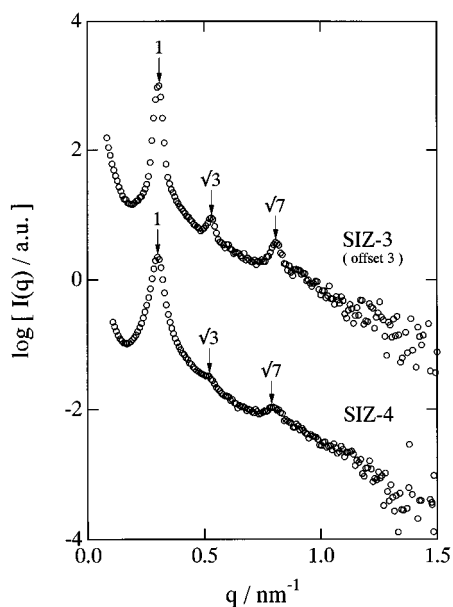


FIG. 1. SAXS profiles shown in the semi-logarithmic plot of the scattering intensity $I(q)$ versus the magnitude of the scattering vector, q , for SIZ-3 and SIZ-4 measured at room temperature. To avoid overlap, the profile for SIZ-3 is shifted vertically by the order of three. Note that the SIZ-3 sample was annealed at 150 °C for 2 h before the SAXS measurement and the SIZ-4 sample was annealed at 110 °C for 26 h.

To avoid overlap, the profile for SIZ-3 was shifted vertically by the order of three. It can be seen that for neat SIZ-3 at least three peaks are discernible, and the q values marked by the arrow are assigned to 1:√3:√7, which correspond to diffraction peaks of hexagonally packed cylinders²³ ($\sqrt{h^2 + hk + k^2}$), and for neat SIZ-4, two higher-order peaks, although they are tiny, are observed and these q values are also assigned to 1:√3:√7. These results are consistent with the well-known fact that the SI diblock copolymer with the volume fraction of PS of either 0.26 (SIZ-4) or 0.65 (SIZ-3) has cylindrical microdomains.^{24,25} Thus it is concluded that both SIZ-3 and SIZ-4 have cylindrical morphologies at temperatures above the glass transition temperature of PS. It should be noted here that the √4 peaks are not discernible in both of the SAXS profiles. The scattering comprises contributions from inter- and intra-particle interferences and those are referred to as *lattice* and *particle* scattering, respectively. Since the particle scattering exhibits alternating constructive and destructive interferences depending on size and shape of the particle, the diffraction peak (lattice scattering peak) disappears when its angular position coincides with that of the destructive interference of the particle scattering. Namely, the extinction condition is governed by the volume fraction of particles in the system. Hashimoto *et al.*²³ calculated structure factors for hexagonally packed cylinders by taking into account of paracrystalline distortion. According to their results, it is found that the √4 peak almost disappears when the volume fraction is around 0.274. For SIZ-4 with $\phi_{PS} = 0.26$, the √4 peak is not observed due to the extinction condition. On the other hand for SIZ-3 with $\phi_{PS} = 0.65$, the extinction condition for the √4 peak is not satisfied. The √3 peak should rather disappear according to the extinction condition for this peak at the volume fraction being roughly

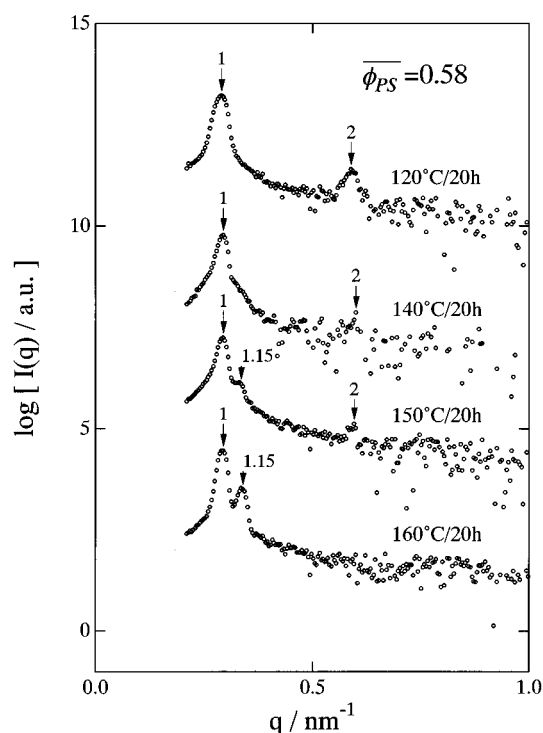


FIG. 2. SAXS profiles measured at room temperature for the binary blend of SIZ-3 and SIZ-4 with $\phi_{PS} = 0.58$ (the overall composition in the unit of volume fraction of polystyrene), annealed at 120, 140, 150, and 160 °C. As-cast samples were annealed at these temperatures for 20 h, then quenched into ice/water mixture, and were subjected to the respective SAXS measurement. Note that those SAXS results were obtained at PLS, Korea. It is also noted that the profiles were shifted vertically to avoid overlaps.

0.326 (and 0.674 complementarily), found by Hashimoto *et al.*²³ The reason why the √4 peak is not observed for SIZ-3 is unclear at present.

Figure 2 shows the SAXS profiles measured at room temperature for the blend with $\phi_{PS} = 0.58$ prepared from two diblock copolymers, SIZ-3 and SIZ-4. Before the SAXS measurements, the samples were annealed at four different temperatures (120, 140, 150, and 160 °C) for 20 h and then quenched into ice/water mixture. These SAXS profiles were obtained at PLS, Korea, and shifted vertically to avoid overlaps. For the blend annealed at 120 °C for 20 h, the relative peak position is expressed by 1:2 which is a clear evidence of a lamellar morphology. While the SIZ-3 and SIZ-4 neat diblock copolymers have the morphologies with PI cylinders and PS cylinders, respectively, the blend comprising these two diblock copolymers turns out to have a lamellar morphology. A similar result has been reported previously for a binary blend of SI diblocks ($\phi_{PS} = 0.26$ and 0.64) with $\phi_{PS} = 0.45$.²⁵ The lamellar morphology is also found in neat SI diblocks when the volume fraction of PS is 0.58.²⁴ This fact suggests that macroscopic phase separation between SIZ-3 and SIZ-4 did not occur in this blend, and furthermore, the morphologies in blends of these two diblocks could be controlled with the overall composition.²⁰ On the other hand, when the blend was annealed at 160 °C for 20 h, the SAXS profile dramatically changed. In addition to the disappearance of the lamellar second-order peak, a sharp peak near by the first-order peak was observed. The q values of these

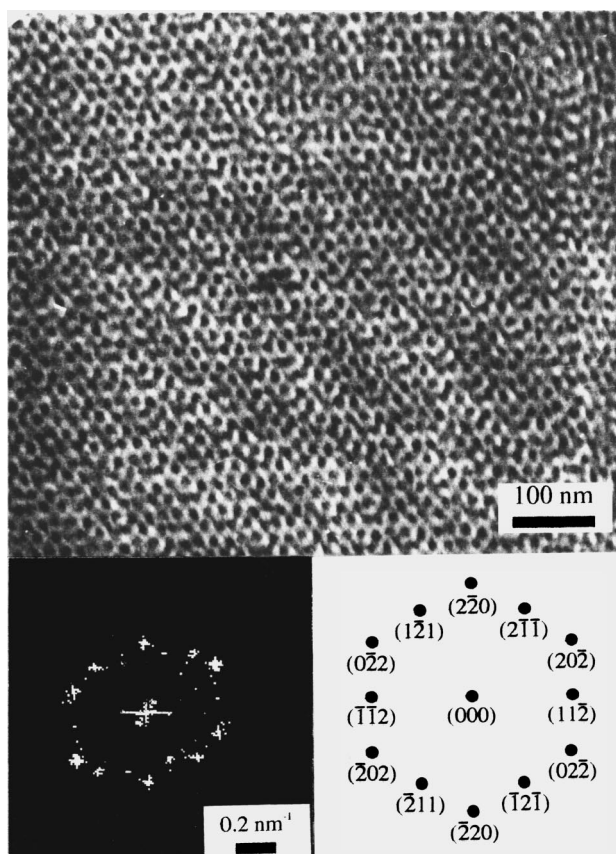


FIG. 3. TEM micrograph for the blend annealed at 200 °C for 20 h. A dark region corresponds to OsO_4 -stained PI phase and bright one is unstained PS phase. The inset is a two-dimensional image of fast Fourier transformation (2D-FFT) for the presented TEM image. Approximately six-fold symmetry about the origin can be found in the 2D-FFT image. A schematic illustration of the diffracted spots with assignment of the Miller indices of a gyroid is shown together in the inset.

peaks can be assigned to 1:1.15 ($=\sqrt{6}:\sqrt{8}$) which are the reflections of (211) and (220) planes of a gyroid structure.⁸ Note here that peak positions for a cubic system are generally expressed by $\sqrt{h^2+k^2+l^2}$. We also found that the intensity ratio of these peaks was 1:0.110. This value is in a better agreement with a theoretical value (1:0.168) for a gyroid morphology than a theoretical prediction (1:0.352) for an ordered bicontinuous double diamond (OBDD) morphology. Note that the ratio of the peak positions is 1:1.22 ($=\sqrt{2}:\sqrt{3}$) for OBDD. Here, the ratios of intensities were calculated by Hajduk *et al.*⁸ for gyroid and OBDD morphologies with 33 vol % of minority phase. These results lead us to conclude that the morphological state of the blend at 160 °C is a gyroid. For the blend annealed at 150 °C for 20 h, although the lamellar second-order peak is still distinct, a tiny side peak is also found at the relative peak position of 1.15, implying that the *L* and *G* phases coexist, because a morphological transition from *L* to *G* occurs at this temperature. For the blend annealed at 140 °C for 20 h, a shoulder can be observed near the relative position of 1.15 corresponding to a gyroid although this is not a sharp peak. This shoulder implies that the annealing time of 20 h was not sufficiently long to observe the side gyroid peak due to very shallow quench (i.e., 140 °C might be very close to the tran-

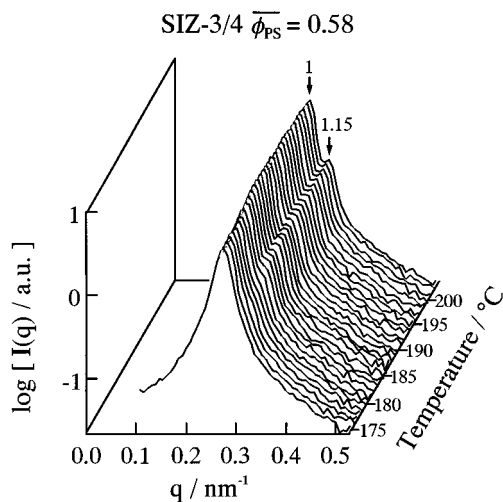


FIG. 4. Change in the SAXS profile with temperature, which is a result of time-resolved SAXS measurements with heating the blend sample at the rate of 2 °C/min.

sition temperature from *L* to *G* phase). Therefore, it is concluded that the blend at 140 °C is near the transition from *L* to *G* phase.

The TEM micrograph for the blend annealed at 200 °C for 20 h is presented in Fig. 3, from which the gyroid morphology is clearly demonstrated. The dark regions correspond to OsO_4 -stained PI phase while the bright ones correspond to unstained PS phase. The inset is a two-dimensional image of fast Fourier transformation (2D-FFT) for the presented TEM projection. Approximately six-fold symmetry about the origin can be found in the 2D-FFT image. A schematic illustration of the diffracted spots with assignment of the Miller indices of gyroid⁸ is shown together in the inset. Thus the experimental 2D-FFT spots can be approximately assigned by the Miller indices of gyroid. Since the gyroid morphology cannot be concluded only from this projection, the result shown in Fig. 3 is a complement to the SAXS results discussed above. From the TEM image with the result of 2D-FFT, the spacing of (211) could be evaluated to be 17.0–19.6 nm, which agrees approximately with the value evaluated from the position of the first-order peak observed for the gyroid phase (see for instance the SAXS profile for 160 °C in Fig. 2, providing the value 21.4 ± 0.3 nm).

In order to study the morphological transition of a specimen when jumped from one temperature to the other, namely *T*-jump experiment, *in situ* observations of the SAXS profiles are most needed. However, in this situation the transition temperature must be known in advance. The reason is that when the destination temperature of the *T*-jump is far from the transition temperature, the morphological change occurs too fast to be followed up experimentally. On the other hand, when the temperature is near the transition temperature, the measurement time becomes too long due to shallow quench. Thus for a sample of which transition temperature is unknown, it is rather effective to perform a conventional temperature sweep with a suitable heating (and/or cooling) rate. Figure 4 exhibits the change in the SAXS profiles with temperature during the heating process with the

rate of 2 °C/min. The evolution of the side peak at the relative position of 1.15 corresponding to the gyroid morphology was clearly displayed. From the results shown in Fig. 4, the peak areas of the first order and the gyroid (220) plane are shown in Fig. 5 as a function of temperature. The width σ_q of the first-order peak (half-width at half-maximum, HWHM) is also shown in Fig. 5. Here, the peak areas were obtained after a computational peak decomposition by using a mathematical expression comprising Gaussian and Lorentzian peak functions with the fraction of the Gaussian component of 0.5.²⁶

It can be seen in Fig. 5 that three regions can be classified. In regime I at temperatures lower than 164 °C, the peak area of the first-order peak decreases but σ_q increases with increasing temperature. Although not shown in Fig. 5, in regime I the areas of the second- and third-order lamellar peaks decreased with increasing temperature, and these two peaks disappeared around 135 °C. In regime II at temperatures between 164 and 188 °C, the peak area of the first-order peak increase with raising temperature. It is interesting to see that σ_q first increases up to ca. 178 °C and then turns to decrease with further increasing temperature. It is also noted that in regime II the side peak corresponding to the gyroid phase is more evident and this peak area increases with increasing temperature. In regime III at temperatures higher than 188 °C, the peak area of the first-order peak decreases with increasing temperature, while the area of the side peak and σ_q remain approximately constant.

From these results, the onset and ending temperatures for the transition from *L* to *G* phase during the heating process are considered as 164 and 188 °C, respectively. In regime I ($T < 164$ °C) the lamellar phase becomes gradually distorted with increasing temperature, and thus the intensity of the first-order peak decreases accordingly. The new gyroid phase was formed from the distorted lamellar phase in regime II ($164 \leq T \leq 188$ °C). The area of the first-order peak in this regime increases due to the formation and ordering of the gyroid phase under the presence of the distorted lamellar phase. The σ_q value of the first-order peak first increases with increasing temperature due to formation of ill-ordered gyroid from the distorted lamellae, but this becomes to decrease later because of the ordering of the gyroid in the later stage of regime II. Namely, it is expected that the lamellar first-order peak becomes broader and weaker with increasing temperature and that the gyroid first-order peak becomes contrary sharper and more intense. However, since the first-order peak for the gyroid overlaps completely to that for the lamellae, the computational peak decomposition was not applicable for the observed apparent first-order peak. No further increase in σ_q of the first-order peak was observed at temperatures higher than 188 °C at which the transition may be completed. However, the area of the first-order peak decreases steadily with increasing temperature in regime III ($T > 188$ °C). This might be attributed to mismatching of the experimental q vector with the direction normal to (211) planes of the preferentially oriented gyroid structures. Under this situation, the intensity of the first-order peak decreases with ordering of the gyroid structures. From the fact that the intensity of the (220) diffraction peak remains approximately

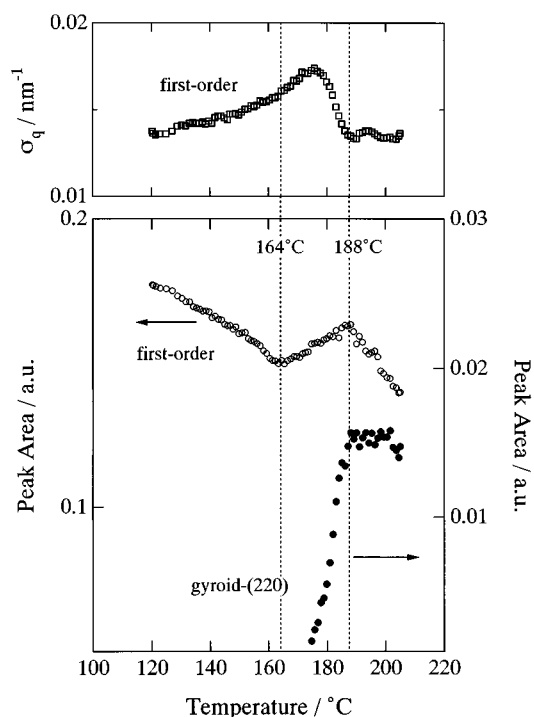


FIG. 5. Peak area and the half-width at half-maximum (HWHM, σ_q) for the first-order peak and the area of the side peak from gyroid [(220) reflection] as a function of temperature. Those values were obtained after computational peak decomposition. Since 164 and 188 °C can be considered as the temperatures of onset and ending of the transition, respectively, three regimes are conventionally considered in terms of these temperatures.

constant in regime III, the matching of the q vector with the direction normal to (220) planes is not best but better than the situation for the (211) reflection.

The temperature range (24 °C) for regime II seems to be quite wide. Moreover, the transition temperature obtained during the heating cycle was 24–48 °C higher than the true transition temperature of 140 °C which was evaluated from the results given in Fig. 2. However, this discrepancy is not striking because of a kinetic effect involved in the different experimental techniques, namely a long time annealing test, i.e., the zero heating rate versus a constant heating process. Similar or even bigger discrepancy due to a kinetic effect has been reported for the phase separation temperature in a binary polymer blend.²⁷ Although the true transition temperature is not quantitatively determined by a conventional temperature sweep experiment during the heating process, one can estimate roughly the transition temperature by this method without conducting a time-consuming thermal annealing test. For instance, since the onset temperature of the transition for this blend was found to be 164 °C during the heating process, one can concentrate the annealing experiment only at temperatures lower than 164 °C, whose results are indeed shown in Fig. 2.

The conventional temperature sweep experiments also allow us to discuss the change in the first-order peak position, q_1 , with temperature, which is shown in Fig. 6. Both in regimes I and III, a monotonous increase of q_1 with temperature is found. Moreover, the scaling relationship $q_1 \sim T^\alpha$ with $\alpha = 0.24$ and 0.34 was confirmed in regimes I and III, respectively. Since q_1 is inversely related to the repeating dis-

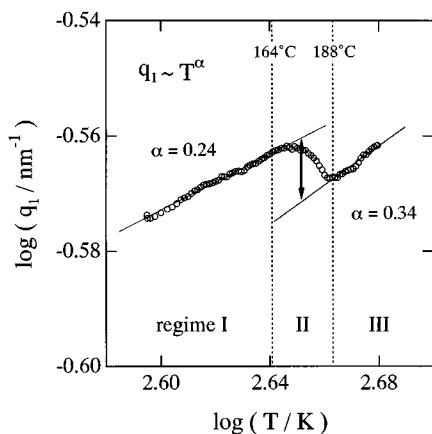


FIG. 6. Change in the peak position, q_1 , for the apparently single first-order peak shown in the double logarithmic plot of q_1 vs. the absolute temperature T . Both in regimes I and III, the scaling relationship $q_1 \sim T^\alpha$ is confirmed with $\alpha = 0.24$ and 0.34 , respectively.

tance of the ordered microdomains, these results indicate that the repeating distance decreases with increasing temperature for both lamellar and gyroid morphologies. It is known that the miscibility between PS and PI blocks increases with temperature due to UCST (upper critical solution temperature) behavior. As a result of enhanced miscibility, the chain dimensions of PS and PI blocks are reduced in the direction normal to the lamellar interface, and hence, the lamellar repeat distance becomes smaller with increasing temperature. The exponent of $\alpha = 0.24$ is approximately consistent with that of $\alpha = 1/3$ reported for a neat SI block copolymer.²⁸

It should be mentioned that the exponent in regime I obtained from a temperature sweep during the heating process may suffer from a nonequilibrium nature of the lamellar morphology above the true transition temperature of 140 °C. However, since the transition from L to G phase takes a long time even at 150 °C, which is deduced from the results given in Fig. 2, the q_1 values for temperatures lower than 150 °C (or $\log T$ is less than 2.63 where T is the absolute temperature) can be adequate enough for the evaluation of the exponent α . Therefore, the exponent of $\alpha = 0.24$ can be reasonable for the lamellar structures. Also, we should carefully examine the reproducibility of the exponent α and the thermoreversibility of the q_1 values in the successive cooling process, since α and q_1 can change with the cooling rate especially for rapid cooling. In regime I, the reverse transition from G to L phase was not found during a cooling process with a rate of 2 °C/min. Therefore, the reproducibility of $\alpha = 0.24$ remains unclear. The reproducibility of α should be examined during the heating and the cooling processes with a suitable rate, say 2 °C/min, within regime I or temperatures less than 150 °C where the morphological transition does not take place during temperature sweep with 2 °C/min. On the other hand, it was confirmed by the separate SAXS experiments that not only the reproducibility of the α ($=0.34$) but also the thermoreversibility of q_1 were confirmed in regime III during the heating and the cooling cycles with the rate of 2 °C/min, suggesting that this rate can be considered to be slow enough to attain an equilibrium

state in terms of the repeating distance of the gyroid structure.

It can be also seen in Fig. 6 that a crossover was found in the behavior of q_1 , implying that the peak position of the lamellar is slightly different from that of the gyroid. However, the difference in q_1 indicated by the double-arrowhead line in Fig. 6 is comparable to an interval of each q value of the SAXS profile, hence it is within an experimental error. Therefore, the change in the peak position during the transition is negligible. This invariance of the peak position upon the transition will be very useful information in order to consider a transition mechanism between L and G phases. It has been shown theoretically by Matsen and Bates²⁹ that a gap in the position of the first-order peak depends on a composition of a diblock copolymer. The gap becomes smaller when the composition (f) is closer to 0.5. Especially, the gap is negligibly small at $f = 0.4$ for a transition between lamellar and gyroid morphologies (and complementarily this fact holds at $f = 0.6$). This is consistent with our experimental result. We also experimentally found that there is no change in the first-order peak position upon the transition from hexagonally-packed cylinders to lamellar structures in a polystyrene-*block*-polybutadiene-*block*-polystyrene triblock copolymer.³

We now discuss the thermoreversibility of the morphological transition between G and L phases. By the conventional temperature sweep experiments, the reverse transition from G to L phase was not found in regime I during a cooling process from ca. 205 °C with a rate of 2 °C/min. It is well known that the transition temperature obtained during the heating process is higher than that obtained during the cooling process when the rate for both processes is the same. For instance, by investigating rheological properties of an SIS triblock copolymer, it was found that the transition from cylindrical (C) to spherical (S) microdomains obtained during the heating process with the rate of 0.5 °C/min occurred at 15 °C higher than that from S to C phases obtained during the cooling process with the same sweep rate.³⁰ Koppi *et al.*³¹ also reported that the transition temperature during the heating process is ca. 15 °C higher than that during the cooling process. Of course, in some cases, the reverse transition during the cooling process is not detected.³² The fact that the blend employed in the present study does not exhibit the reverse transition from G to L phases may be therefore attributed to the hysteresis effect between the cooling and heating processes. More careful examinations are currently in progress to check the thermoreversibility of the transition between L and G phases.

IV. CONCLUDING REMARKS

We presented in this paper clear evidence of the morphological transition from lamella at a lower temperature to gyroid phase at a higher temperature. This transition is different from thermally induced transition of kinetically locked morphology due to vitrification of PS matrix. It was found by a separate experiment with conducting a considerably long time annealing that the lamellar morphology was stable at 140 °C which is well above the glass transition temperature of PS. A very important result with respect to change in the

position of the first-order peak upon the transition was obtained from the time-resolved SAXS measurement with a temperature sweep. The fact that the peak position is conserved upon the transition will be useful information in order to construct a model of the transition between *L* and *G*. Moreover, the result shown in Fig. 6 is also useful to design *T*-jump experiments, i.e., to choose initial and final temperatures of *T*-jump, since a suitable temperature range for the time-resolved SAXS measurements may be restricted in a narrow range, as claimed above. An initial temperature in the range of $140 \leq T \leq 160$ °C and a final temperature in the range of $165 \leq T \leq 190$ °C presumably deserve good choice. Based on the preliminary results presented here, *T*-jump experiments are planned as a continuation of this work.

The thermoreversibility of the transition is not yet confirmed in this study. However, it does not necessarily mean that the lamellar morphology is not stable at a lower temperature, because the reverse transition from *G* to *L* can be considered to be kinetically prohibited more than the forward transition (*L* to *G*) in the binary blends of diblock copolymers. Note that the self-consistent field theory predicted stability of the gyroid phase for a neat diblock copolymer at the compositional range around 0.58.¹¹

ACKNOWLEDGMENTS

We thank T. Fukui (Nippon Zeon Co., Ltd.) for kindly supplying the SI samples. This work is financially supported by Grant-in-Aid from Japan Ministry of Education, Science, Culture, and Sports with 07236228 granted to S.N. (Priority Areas "Cooperative Phenomena in Complex Liquids") and 08751048 granted to S.S. The time-resolved SAXS measurements were conducted under approval of the Photon Factory Advisory Committee (Proposal Number 94G284). Synchrotron SAXS experiments were in part performed at the PLS, which was supported by Ministry of Science and Technology (MOST) and Pohang Iron & Steel Co. (POSCO, Korea).

¹S. Sakurai, Trends Polym. Sci. **3**, 90 (1995).

²S. Sakurai, H. Kawada, T. Hashimoto, and L. J. Fetters, Proc. Japan Acad. Ser. B **69**, 13 (1993).

³S. Sakurai, T. Momii, K. Taie, M. Shibayama, S. Nomura, and T. Hashimoto, Macromolecules **26**, 485 (1993).

⁴S. Sakurai, H. Kawada, T. Hashimoto, and L. J. Fetters, Macromolecules **26**, 5796 (1993).

⁵S. Sakurai, K. Taie, S. Nomura, T. Shiwaku, and T. Hashimoto, ACS Polymer Preprints **35**, 594 (1994).

⁶F. S. Bates, M. F. Schulz, A. K. Khandpur, S. Förster, J. H. Rosedale, K. Almdal, and K. Mortensen, Faraday Discuss. **98**, 7 (1994).

⁷D. A. Hajduk, S. M. Gruner, P. Rangarajan, R. A. Register, L. J. Fetters, C. Honeker, R. J. Albalak, and E. L. Thomas, Macromolecules **27**, 490 (1994).

⁸D. A. Hajduk, P. E. Harper, S. M. Gruner, C. C. Honeker, G. Kim, E. L. Thomas, and L. J. Fetters, Macromolecules **27**, 4063 (1994).

⁹S. Sakurai, T. Hashimoto, and L. J. Fetters, Macromolecules **29**, 740 (1996).

¹⁰S. Sakurai, H. Umeda, K. Taie, and S. Nomura, J. Chem. Phys. **105**, 8902 (1996).

¹¹M. W. Matsen and F. S. Bates, Macromolecules **29**, 1091 (1996).

¹²S. Sakurai and S. Nomura, Polymer **38**, 4103 (1997), and references therein.

¹³T. Hashimoto, H. Tanaka, and H. Hasegawa, Macromolecules **23**, 4378 (1990).

¹⁴P. K. Janert and M. Schick, Phys. Rev. E **54**, R33 (1996).

¹⁵T. Hashimoto, K. Yamasaki, S. Koizumi, and H. Hasegawa, Macromolecules **26**, 2895 (1993).

¹⁶J. Zhao, B. Majumdar, M. F. Schulz, F. S. Bates, K. Almdal, K. Mortensen, D. A. Hajduk, and S. M. Gruner, Macromolecules **29**, 1204 (1996).

¹⁷A.-C. Shi and J. Noolandi, Macromolecules **28**, 3103 (1995).

¹⁸M. W. Matsen and F. S. Bates, Macromolecules **28**, 7298 (1995).

¹⁹S. Sakurai, H. Umeda, A. Yoshida, and S. Nomura, Macromolecules **30**, 7614 (1997).

²⁰S. Sakurai, H. Irie, H. Umeda, S. Nomura, H. H. Lee, and J. K. Kim, Macromolecules (in press).

²¹L. J. Fetters, D. J. Lohse, D. Richter, T. A. Witten, and A. Zirkel, Macromolecules **27**, 4639 (1994).

²²B. J. Park, S. Y. Rah, Y. J. Park, and K. B. Lee, Rev. Sci. Instrum. **66**, 1722 (1995).

²³T. Hashimoto, T. Kawamura, M. Harada, and H. Tanaka, Macromolecules **27**, 3063 (1994).

²⁴H. Hasegawa, H. Tanaka, K. Yamasaki, and T. Hashimoto, Macromolecules **20**, 1651 (1987).

²⁵S. Koizumi, H. Hasegawa, and T. Hashimoto, Macromolecules **27**, 4371 (1994).

²⁶In order to express a single diffraction peak, we applied a mathematical expression comprising Gaussian and Lorentzian peak functions with the fraction of the Gaussian component of 0.5. It is simply because the combined expression was found to fit a diffraction peak well (Ref. 10). Namely, we have only such the technical reason. We do not mean that the Gaussian type was used for a peak from one phase (e.g., lamellae) while the Lorentzian type was used for a peak from the other phase (e.g., gyroid). For both peaks from lamellae and gyroid, the combination of Gauss and Lorentz with the Gaussian fraction of 0.5 was equally employed.

²⁷J. Maruta, T. Ougizawa, and T. Inoue, Polymer **29**, 2056 (1988).

²⁸T. Hashimoto, M. Shibayama, and H. Kawai, Macromolecules **13**, 1237 (1980).

²⁹M. W. Matsen and F. S. Bates, J. Chem. Phys. **106**, 2436 (1997).

³⁰J. K. Kim, H. H. Lee, M. Ree, K. B. Lee, and Y. J. Park, Macromol. Chem. Phys. (in press).

³¹K. A. Koppi, M. Tirrell, F. S. Bates, K. Almdal, and K. Mortensen, J. Rheol. **38**, 999 (1994).

³²S. Förster, A. K. Khandpur, J. Zhao, F. S. Bates, I. W. Hamley, A. J. Ryan, and W. Bras, Macromolecules **27**, 6922 (1994).